Transworld Research Network
37/661 (2), Fort P.O., Trivandrum-695 023, Kerala, India

Plasma Physics Applied, 2006: 73-110 ISBN: 81-7895-230-0
Editor: Crockett Grabbe

5 Dusty plasmas and applications in space and industry

Robert L. Merlino
Department of Physics and Astronomy, The University of Iowa
Iowa City, IA 52242, USA

Abstract

A dusty plasma is an ionized gas containing dust particles, with sizes ranging from tens of nanometers to hundreds of microns. The interaction of the dust particles with the plasma and ambient environment results in a charging of the dust grains. This Chapter summarizes our basic knowledge of dusty plasmas with applications in space, industry and the laboratory. The Introduction (Section 1) provides several examples of dusty plasmas, taken from astrophysics, the solar system, earth, industry and the laboratory. The basic physical principles governing the charging mechanisms and behavior of dust particles is presented in Section 2. Section 3 discusses

Correspondence/Reprint request: Dr. Robert L. Merlino, Department of Physics and Astronomy, The University of Iowa, Iowa City, IA 52242, USA. E-mail: robert-merlino@uiowa.edu

examples of dusty plasmas in the solar system and earth. Section 4 describes examples of dusty plasmas in industry, and in particular the problem of dust formation and resulting contamination in plasma processing devices used to produce semiconductor devices. Technologically exciting new applications of dusty plasmas are also discussed. Section 5 reviews the basic laboratory devices that have been developed to study dusty plasmas. Some of the most interesting discoveries made in these devices, such as the formation of dust lattice structures (Coulomb crystals) are also described. A brief review of the results of novel experiments in dusty plasmas performed in the microgravity environment onboard the International Space Station (ISS) is presented. Finally, the problem of dust in fusion devices is outlined.

1. Introduction

Dusty plasmas are ionized gases that contain particulates of condensed matter. These particles may have sizes ranging from tens of nanometers to hundreds of microns. They may be in the shape of spheres or rods or irregularly shaped pancakes. They may be composed of dielectric, e.g. SiO_2 or Al_2O_3, or conducting materials. Although the particles are commonly solid, they might also be fluffy ice crystals or even liquid droplets. They are typically much more massive than the plasma electrons and ions. For example, a solid spherical particle of radius 1 μm of material of mass density 2000 kg/m^3 will have a mass of 8×10^{-15} kg, corresponding to roughly 5 trillion proton masses. What makes dusty plasmas interesting and technologically important is the fact that the dust particles acquire an electric charge in the plasma, typically a negative charge. For example, the 1 μm radius spherical dust particle immersed in a plasma with room temperature ions and 1 eV electrons will acquire a charge, $Q \approx 3\times10^{-16}$ C, corresponding to a Q/e of roughly 2000, where e is the elementary electric charge. The dynamics of these massive charged particles occurs on considerably slower time scales than the ordinary plasma ions, since their charge to mass ratio is orders of magnitude smaller that the corresponding (e/m) of either the electrons or ions.

Where are dusty plasmas found? Dust turns out to be ubiquitous in cosmic plasmas, planetary plasmas, plasmas near the earth and plasmas in the laboratory. In fact, one may speculate that except in the hottest regions of fusion plasmas where dust particles would not survive, most plasmas are dusty plasmas in the sense that some dust particles may be present. As a guide, one distinguishes two cases in which: (1) there are only few isolated (non-interacting) dust particles, so that they have little if any influence on the plasma, and (2) there are a very large number of particles in the plasma so that their presence actually alters the properties and behavior of the plasma. In case (1) the particles are charged by their interaction with the plasma but do not change the plasma in any observable way. On the other hand, case (2) corresponds to the situation in which the charged dust is a *component* of the plasma, subject to the collective interactions that distinguishes an ionized gas from a neutral gas. Case (2) is what is normally defined as a "dusty plasma". In Table 1 several examples of dusty plasmas are given under a broad classification scheme which distinguishes naturally occurring dusty plasmas and man-made dusty plasmas, i.e., dust plasmas produced in connection with some human activity. The naturally occurring dusty plasmas are further classified by their location in cosmic settings, the solar system, or around the earth. The man-made dusty plasmas include examples of ones produced either intentionally (by introducing dust in plasmas to study its properties and effects) or unintentionally as in fusion devices.

That an ordinary flame contains dust particles (soot) will come as no surprise, but the fact that it can be considered a plasma is intriguing. In fact, it is the presence of the un-burnt carbon particles that makes it a plasma. Thermionic emission of electrons from the soot particles, which are heated to above 1000°C in a candle flame, raises the degree of ionization by several orders of magnitude, qualifying it for the designation as *plasma*. On a much larger scale it is well-known that comets generally have two tails. One tail is due to the comet's dust particles, the other is due to ionized gas from the comet coma.

Table 1. Dusty plasmas.

"Naturally Occurring"	**"Man-made"**
Cosmic • Solar nebulae • Planetary nebulae • Supernova shells • Interplanetary medium • Molecular clouds • Circumsolar rings • Asteroids ***Solar system*** • Cometary tails and comae • Planetary ring systems – Saturn's rings • Dust streams ejected from Jupiter • Zodiacal light ***Earth*** • Lightening discharges • Volcanoes • Meteoric dust • Noctilucent clouds in the mesosphere • "moon clouds"	• Ordinary flames • Rocket exhaust • Dust on surfaces in space (space station) • Dust in fusion devices • Thermonuclear fireballs • Atmospheric aerosols • Dust precipitators used to remove • pollution from smoke stacks • Plasmas used for microelectronic fabrication, e.g. semiconductor chips, solar cells and flat panel displays • Plasma Enhanced Chemical Vapor Deposition (PECVD) technologies • Dusty plasma devices (DPDs) used to produce and study dusty plasmas in the laboratory

Near the coma these tails are not distinct but overlap forming a dusty plasma. A complete analysis of certain dynamical features observed in comet tails thus requires application of dusty plasma physics. The importance of dust has long been known in astrophysics, as it is very common throughout the universe and accounts for a good fraction of all its solid matter. The evolution of the solar system into its present state is thought to have proceeded from a stage of solid matter in the form of dust particles, with larger objects forming through coagulation of the dust particles. Since the gaseous component of the solar nebula was very likely at least partially ionized, the initial evolution from dust to larger objects undoubtedly also involved dusty plasma physics.

The reader is referred to several excellent review articles and monographs on various aspects of dusty plasmas. Anyone who is a newcomer to this field is encouraged to start with the review article by my former colleague Chris Goertz, on "Dusty Plasmas in the Solar System" [1]. A summary of progress in dust plasma research from the perspective of one of the founders and leading researchers in this field appears in an article by Asoka Mendis [2]. Another leading figure in this field, Padma Shukla, has provided a comprehensive review article focusing on collective processes in dusty plasmas [3]. The community has also been fortunate to have most of the basic principles of dusty plasmas set out very clearly in the monograph of Shukla and Mamun [4]. Technological aspects of dusty plasmas have been thoroughly compiled in a book edited by André Bouchoule [5]. I also point to review articles dealing with certain aspects of dusty plasmas such as dynamical processes in dusty plasmas [6], and waves and instabilities in dusty plasmas [7]. An excellent article in Physics Reports published in December 2005, reviews the field of dusty plasmas and provides some perspective on its current status and open issues [8]. The second edition of the textbook by Michael Lieberman and Allan Lichtenberg, *Principles of Plasma Discharges and Materials Processing,* contains full discussions of the devices used in plasma processing, with an entire chapter devoted to dusty plasma physics [9]. Finally, a Physics Today article intended for a more general audience, including undergraduate physics students, was written by this author and his colleague John Goree [10].

2. Dusty plasma physics

Consideration of the entries in Table 1 reveals the wide range of phenomena in which dust plays a role. It might at first seem odd that a connection exists between the rings of Saturn and industrial devices used to manufacture semiconductors, but the commonality lies in the presence of charged dust particles. Before describing some of the examples listed in Table 1 in more detail, we give a brief discussion of the basic principles of dusty plasma physics that are required for an understanding of much of the phenomena presented in Table 1.

A. The charge on a dust grain in a plasma

We consider the case of an isolated spherical dust grain of radius a in a plasma having a Debye shielding length λ_D, where a << λ_D. If many dust grains are present, they may still be considered isolated if the intergrain spacing d >>λ_D. Since the dust grain is electrically floating, it draws no net current from the plasma. The charge, Q on a dust grain must then satisfy the charging equation

$$\frac{dQ}{dt} = \frac{d}{dt} \cdot \left(C\phi_s\right) = \sum_j I_j = 0 \qquad [1]$$

where C is the grain capacitance, which for spherical grains is given by

$$C = 4\pi\varepsilon_o a, \qquad [2]$$

and

$$\phi_s \equiv V_s - V_p \qquad [3]$$

is the grain surface potential, V_s, relative to the ambient plasma potential, V_p, and I_j are the various currents collected by the grain due to: electrons and ions, secondary electron emission, and photoelectric emission. The currents depend both on the properties of the dust grain and on the ambient plasma conditions. For example, the electron and ion currents to the grain, which are the most important ones under typical laboratory dusty plasma conditions, depend on the size of the grains, the velocity distributions of the plasma particles and on the potential of the grain relative to the plasma ϕ_s. Under conditions where the currents due to photoelectron emission and secondary emission can be neglected, the dust grain charge is due to the collection of electrons and ions. Since the electrons typically move considerably faster than the positive ions, electrons are first collected by the grain, and the grain acquires a negative potential relative to the plasma so as to repel further electron collection and enhance the positive ion collection until the balance is achieved with the net current, $I_e + I_i = 0$, where I_e and I_i are the electron and ion currents, respectively. For $\phi_s < 0$, these currents are given by [4]

$$I_e = -\frac{en_e}{4}\left(\frac{8kT_e}{\pi m_e}\right)^{\frac{1}{2}} \exp\left(\frac{e\phi_s}{kT_e}\right) 4\pi a^2, \qquad [4a]$$

$$I_i = \frac{en_i}{4}\left(\frac{8kT_i}{\pi m_i}\right)^{\frac{1}{2}} \left(1 - \frac{e\phi_s}{kT_i}\right) 4\pi a^2, \qquad [4b]$$

where n_e and n_i are the electron and ion densities, T_e and T_i are the electron and ion temperatures, and m_e and m_i are the electron and ion masses, respectively. The ion current is taken from the orbital-motion-limited (OML) model [11]. The relative dust surface potential, ϕ_s, is then determined by numerical solution of the transcendental equation that results when Eqs. 4a and 4b are inserted into Eq. 1. Assuming quasineutrality, $n_e = n_i$, in a plasma with argon ions, Ar^+ at $T_i = 0.025\ eV$ and electrons with $T_e = 1\ eV$, we obtain $\phi_s = -2.74\ V$. For a given dust grain radius a, the charge is then calculated from $Q = 4\pi\varepsilon_o a\ \phi_s$. Fig. 1 shows a plot of the normalized relative dust surface potential, ϕ_s / kT_e, versus the ratio T_e/T_i for a plasma of H^+ ions and Ar^+ ions. For $T_e/T_i = 1$, we see that the potential (and thus the dust charge) is more negative for the plasma with the more massive positive ion, since the relative electron mobility is larger in the Ar^+ plasma.

If the electrons and ions impinging on the dust particles are very energetic, they may cause a release of secondary electrons. In these cases an additional current due to the secondary electrons must be included in the computation of the dust surface potential. Typically secondary emission is not significant unless the energy of the impinging electrons is on the order of several tens of eV. Ion induced secondary electron emission does not become significant until ion energies in excess of 1 keV hit the dust.

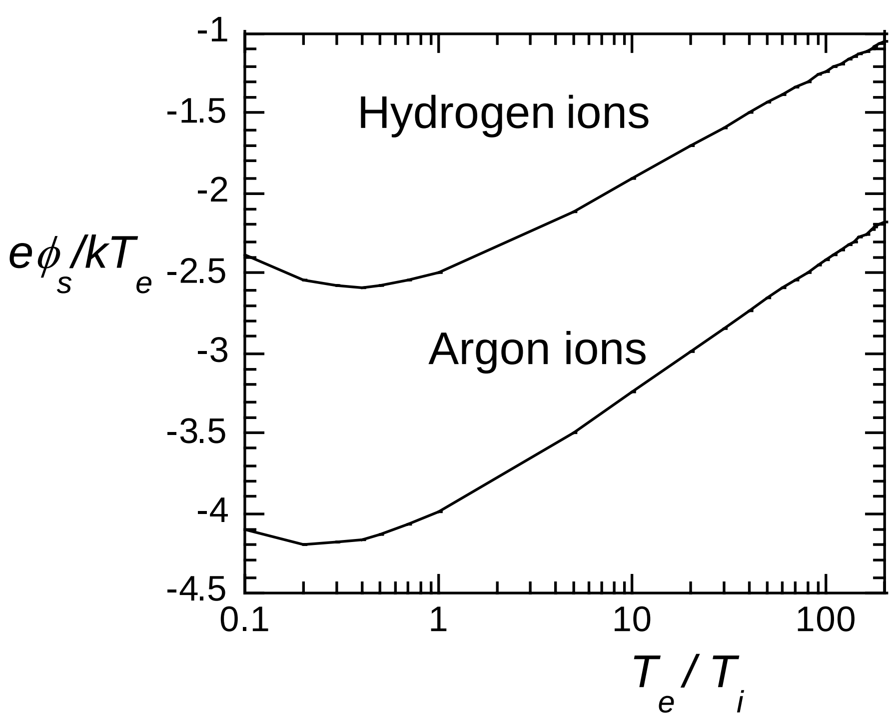

Figure 1. The normalized dust surface potential (relative to the plasma potential vs. the ratio of electron to ion temperature for plasmas with hydrogen ions and argon ions.

If a flux of photons with energy larger than the work function of the dust material is incident on a dust grain, photoelectrons are emitted from the dust. Since typical work functions for thermionic emission are ~ *2 – 5 eV*, photoemission becomes important when the dust is exposed to UV radiation. Photoemission can be produced by sunlight falling on dust, aerosols or ice crystals in the upper atmosphere. Photoelectric charging of dust can be the dominant charging mechanism for dust in many astrophysical settings. In the absence of plasma, photoelectric charging will lead to dust with a positive charge. If dust is present in a plasma while exposed to UV radiation, then charging currents do to electrons, ions and photoelectrons must be used in the computation of the dust surface potential. Photoelectric charging was apparently responsible for the Apollo 11 astronauts' reports of "Moon clouds" – a "weird glow" seen on the Moon's horizon. The Moon dust particles can be photoelectrically charged and levitated above the Moon's surface. The "clouds" were apparently visible to the astronauts in reflected sunlight.

This last example highlights one important aspect of dusty plasmas – dust grains with sizes on the order of microns or larger can be visually detected in a plasma. By illuminating the dust particles with laser light, the motion of individual dust grains can be recorded by CCD cameras for later analysis. Thus it has been possible for researchers to obtain the complete phase space (position and velocity) mapping of dust particles in a plasma as a function of time. This type of detailed measurement is not possible in ordinary plasmas.

B. The forces on a dust grain in a plasma

Knowledge of the various forces acting on dust particles in a plasma is necessary for an understanding of their dynamics and transport. The various forces scale differently with particle size so that the force balance, which determines where the particles are trapped, depends sensitively on location within the plasma. The discussion of these forces follows closely the treatment of Barnes et. al. [12], on the transport of dust particles in glow–discharge plasmas.

1.Force of gravity, F_g.— Except under microgravity conditions, a dust particle is subject to gravity with a force that is proportional to its mass and thus can be written as

$$F_g = m_d g = \frac{4}{3}\pi a^3 \rho_d g \qquad [5]$$

where g is the local acceleration due to gravity and ρ_d is the mass density of the particle. For most solid materials, ρ_d ~ 2000 kg/m^3. For submicron particles, this force can sometimes be neglected, but for micron sized or larger particles, this can often be the dominant force which usually limits the time during which the particle resides in the plasma.

2. The electric force F_e.— At a location in the plasma having an electric field E, the electric force, acting on dust particles of charge Q is

$$F_e = QE \qquad [6]$$

The electric field is much larger in sheaths adjacent to the plasma–wall boundary and much smaller in the bulk of the plasma. For example, micron sized particles in typical rf parallel plate glow discharge plasmas, are found to reside near the lower (negative) electrode where the relatively large downward directed electric sheath field provides an upward electric force that balances the weight of the particle, allowing it to levitate there indefinitely.

3. Neutral drag force F_n.— This force results from collisions with the background neutral gas atoms or molecules and is therefore proportional to the neutral pressure in the vacuum chamber. F_n is given approximately by

$$F_n = Nm_n v_{dn}^2 \pi a^2 \qquad [7]$$

where N is the neutral density, m_n is the mass of the neutral atoms (or molecules), and v_{dn} is the average relative velocity between the neutrals and dust particle. If the dust particle is drifting, this force is in the direction opposite to its motion, resulting in a damping force on the dust particles. Alternately, if there is a flow of neutral gas, there is a net transfer of momentum to the dust in the direction of the neutral flow.

4. Thermophoretic force, F_{th}.— This force occurs if there is a temperature gradient in the neutral gas in the plasma, and is in the direction opposite to that of the temperature gradient. The origin of this force is the fact that gas molecules from the hotter portion of the gas transfer more momentum than gas molecules from the colder side of the gas. This force is given approximately by

$$F_{th} = \frac{16\sqrt{\pi}}{15} \frac{a^2 \kappa_T}{v_{T,n}} \nabla T_n \qquad [8]$$

where, $v_{T,n}$ is the thermal speed of the neutral gas, κ_T is the translational part of the thermal conductivity, and T_n is the temperature of the neutrals. The thermophoretic force can be induced by heating of one of the electrodes in the discharge. The resulting temperature gradient can then be used to balance the forced of gravity on the dust particles [13].

5. Ion drag force, F_i.— The ion drag force is due to the transfer of momentum to dust particles by collisions with ions. The ion impact may be due to drifting ions driven by an electric field in the plasma. The electric field thus influences the dust particles either directly through the electric force, or indirectly through the ion drag force. The ion drag force consists of two parts: the collection force, F_{ic} and the orbit force, F_{io}, so that

$$F_i = F_{ic} + F_{io} \quad [9]$$

The collection force is due to momentum transfer from all ions that are collected by the particle. Each ion transfers its momentum $m_i v_i$, so that this force is given by

$$F_{ic} = n_i m_i v_i v_s \pi b_c^2 \quad [10]$$

where n_i is the ion density, m_i is the mass of the ions, v_i is the ion drift speed, v_s is the mean speed of ions approaching the particle, given by

$$v_s = \left(\frac{8kT_i}{\pi m_i} + v_i^2 \right)^{\frac{1}{2}} \quad [11]$$

and

$$b_c = a\left(1 - \frac{2e\phi_s}{m_i v_s^2} \right)^{\frac{1}{2}} \quad [12]$$

is the collision impact parameter based on orbit–motion–limited (OML) theory. The orbit force is due to transfer of momentum by ions that are deflected by the particle but do not reach the particle's surface and can be written as

$$F_{io} = 4\pi n_i m_i v_i v_s b_{\pi/2}^2 \Gamma \quad [13]$$

where

$$b_{\pi/2} = \frac{eQ}{4\pi\varepsilon_o m_i v_s^2} \quad [14]$$

is the impact parameter for 90° deflections and

$$\Gamma = \frac{1}{2}\ln\left(\frac{\lambda_D^2 + b_{\pi/2}^2}{b_c^2 + b_{\pi/2}^2} \right) \quad [15]$$

is the Coulomb logarithm integrated over the interval from b_c to λ_D.

This theory for the ion drag force was obtained under the assumption that no interaction with the dust particle occurs for ions approaching outside the Debye length of the particle. Significant extentions to this theory have been presented by Khrapak et al [14].

C. Weakly vs. strongly coupled dusty plasmas

An important consideration in the analysis of dusty plasmas is whether or not the particles are in the weakly or strongly coupled state. The designation as weakly or strongly coupled refers to the issue of whether the particles' average potential energy due to nearest neighbor interactions is smaller or larger than their average thermal energy. For a non–dusty plasma, the electrons and ions are typically in a state in which the average interaction energy is much less than the average thermal energy, a situation that is often taken as a defining characteristic of a plasma. However, the dust particles in a dusty plasma can acquire substantial charges which greatly enhances the average potential energy due to nearest neighbor interactions. The possibility of finding dust in the strongly coupled state is determined by its Coulomb coupling parameter, Γ defined as the ratio of the interparticle Coulomb potential energy to the (thermal) kinetic energy of the particles

$$\Gamma = \frac{Q^2}{4\pi\varepsilon_o d\, kT_d} \qquad [16]$$

where d is the average interparticle spacing, which can be estimated as $d = \left[4\pi n_d / 3\right]^{-1/3}$, n_d is the dust density and T_d is the dust temperature.

For example, in a dusty plasma with Q = 5000 e, kT_d = 0.05 eV, $n_d = 10^{10}$ m^{-3} (d = 464 μm), we find that Γ = 1500 >> 1. Ikezi [15] has argued that when Γ exceeds some critical value (~170), the dust particles will be arranged in an orderly lattice termed either a plasma crystal or Coulomb crystal. The experimental observation of these Coulomb crystals in 1994 by several groups was one of the most important discoveries in dusty plasmas and will be discussed in Section 5 B.

D. Formation and growth of dust particles in a plasma

A novel aspect of plasmas that contain chemically active species is that dust particles can actually be formed and grow in size. This is particularly true of plasma devices in the semiconductor processing industry in which mixtures of gases such as silane, SiH_4, oxygen, O_2, and, Ar are used in the fabrication of electronic microchips. Dust particles can also form in plasmas when atoms or molecules from either the walls or electrodes are sputtered into the plasma by ion or electron bombardment. For example, in parallel plate rf discharges using carbon electrodes, carbon atoms are sputtered off of the electrode which eventually coagulate into larger clusters [16].

Plasma processing devices used for manufacturing silicon wafers typically employ a parallel plate arrangement in which 13.56 MHz rf power is applied to the lower electrode to form the plasma. Etching of the wafer requires a reactive species such as silane introduced along with a buffer gas such as argon. Plasma assisted gas phase chemical reactions lead to the formation of SiH_2 most likely through the reaction $e^- + SiH_4 \rightarrow (SiH_4)^* \rightarrow SiH_2 + 2H$. Collisions of SiH_4 with electrons leads to a vibrationally excited state which then dissociates into SiH_2. Fig. 2 shows an example of particle growth data taken in a parallel plate rf reactor system operating with silane [17]. Over time, the particle sizes increase while the density of particles decreases.

Particle growth in plasmas is thought to proceed via several steps: (i) nucleation, (ii) coagulation, and (iii) surface growth. Nucleation is essentially a series of chemical reactions in the gas phase in which parent gas monomers are transformed into macromolecules and small clusters. Nucleation generally leads to the formation of particles of 0.2 nm size which have only a few elementary charges. This process is known as gas phase polymerization. When a critical number of primary clusters are formed, the process of agglomeration or coagulation is triggered and the particles grow rapidly in size to about 50 nm. Coagulation is defined as the process in which two particles collide to

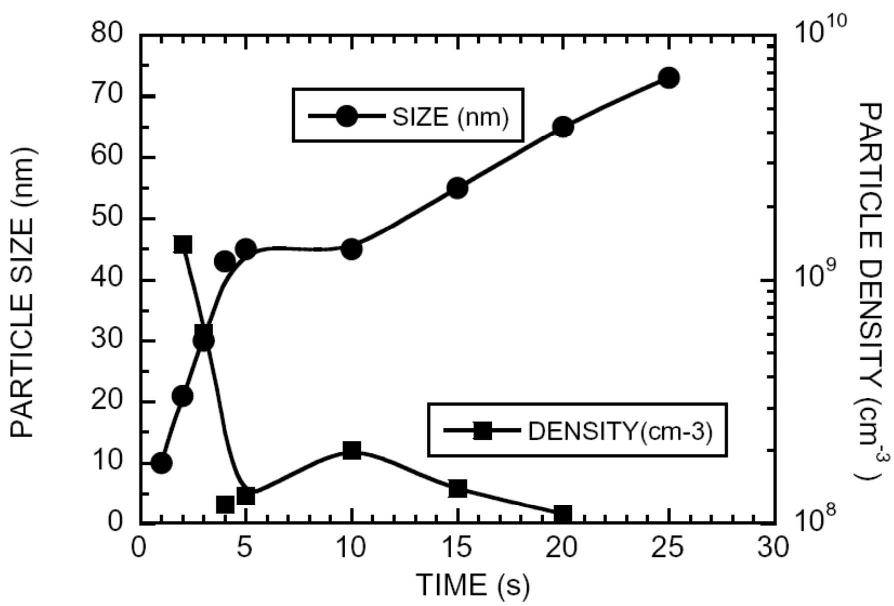

Figure 2. Growth of particles in an rf-produced silane-argon plasma. The particle size (solid circles) increases with time, while the density of particles (solid squares) decreases with time. (adapted from [17])

form a larger particle. As the particle size grows they collect more and more negative charge which impedes further coagulation due to the mutual Coulomb repulsion of the particles. Following the agglomeration phase, the particles continue to grow by the process of surface growth. Surface growth proceeds as plasma radicals begin sticking to the existing particles. The particles now behave as small substrates onto which additional layers deposit. This phase continues until the particles reach micron size, at which point gravity causes them to fall out of the plasma. A schematic representation of the particle growth process as it proceeds through each phase is shown in Fig. 3.

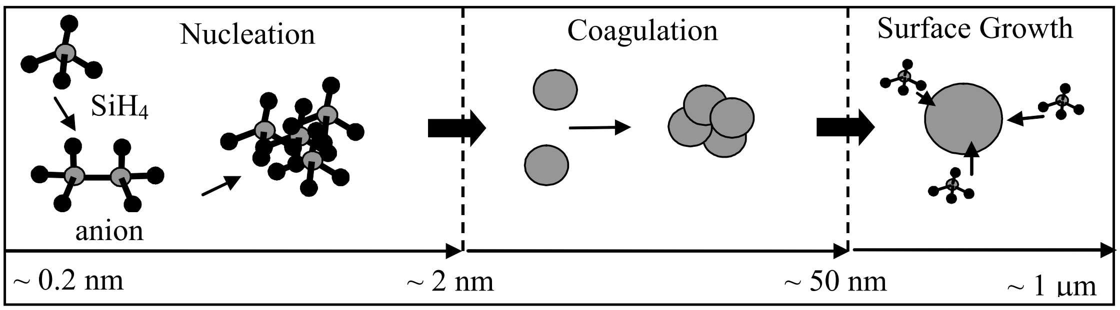

Figure 3. Schematic diagram showing the three phases of particle growth in reactive silane plasmas. (adapted from [18])

3. Dusty plasmas in the solar system and on earth

In this section, two examples of unexpected discoveries of dusty plasmas in the solar system will be presented – the curious observation of spokes in Saturn's B ring, and dust streams ejected from Jupiter. Also, two examples of dusty plasma effects occurring on or near Earth are also described - the silvery-blue-shining noctilucent clouds and associated polar mesospheric summer echoes, and what I will refer to as 'snowy plasma' – the triboelectric charging of blowing snow.

Of course there are many examples of dusty plasmas in astrophysics and the reader is referred to the pioneering work by Lyman Spitzer [19] for more details. Lyman Spitzer along with Hannes Alfvén [20] recognized that the dust in the Universe was not merely a hindrance to optical observations, but that it was an essential component of the Universe, out of which larger objects, such as planets, emerge. Lyman Spitzer provided some of the basic framework needed to understand first that the dust would likely be charged and second, how to compute the potential (and charge) on a dust grain.

A. Spokes in Saturn's B ring

One of the most important and exciting events in the field of dusty plasmas occurred in early 1980 during the Voyager 2 flyby of the planet Saturn. Images (see Fig. 4 a,b) taken of Saturn's rings revealed a pattern of nearly radial "spokes" rotating around the outer portion of the dense B ring [21]. As the spacecraft approached the planet, the spokes first appeared dark against the bright background. But as Voyager 2 withdrew from Saturn, the spokes appeared brighter than the material around them. The observation that the spoke material scatters light more effectively in the forward direction indicated that the material was fine dust, on the order of 0.5 μm. Perhaps the most unexpected feature of the observations was that these wispy features formed remarkably quickly, with new spokes appearing in as little as five minutes. The ephemeral nature of the spokes, with dynamical timescales on the order of minutes immediately indicated that they could not be explained by gravitational forces alone. Their formation and dynamics must be controlled by electromagnetic forces, and thus the particles must be charged.

The spokes would not be observed again until 1996 when the Hubble Space Telescope (HST) targeted Saturn and made an extensive series of observations of the rings [22]. In July 2004 the Cassini spacecraft was inserted into a durable orbit around Saturn. Cassini was equipped with imagers having better spatial and temporal resolution than Voyager, and thus planetary scientists and plasma physicists looked forward to new and improved images of the spokes with detail that would provide a better basis for understanding their origin. The first set of spoke observations by Cassini were made in September 2005, and are shown in Fig. 4 (c). Although it was initially expected that the spoke would be seen by

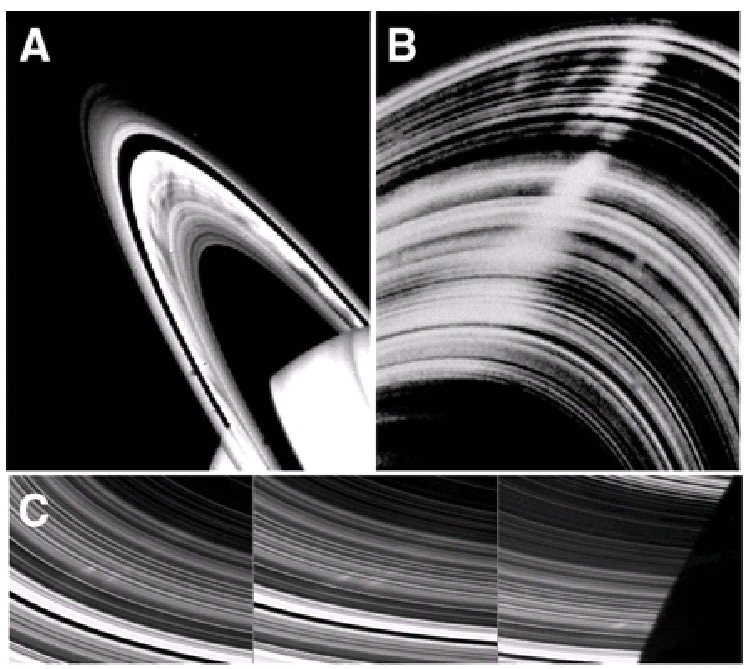

Figure 4. Spokes in Saturn's B ring observed in 1980 by Voyager 2 (a) and (b), and in 2005 by Cassini (c). The three Cassini images cover a span of 27 min.

Cassini much earlier, it is now believed [23] that the charging environment above the rings prevented the formation of spokes until very recently. The prospects for observing spokes should be excellent by the end of 2006 due to a more favorable formation and viewing geometry.

The observation of the spokes in the early 80’s was likely responsible for the explosion of activity in dusty plasmas. Suddenly, dust was not just of interest to astrophysicists but to planetary scientists and plasma physicists as well. So what causes the spokes? Electrostatic interactions were first considered as a likely explanation. The scenario of spoke formation requires a transient event that would charge the grains to sufficiently high potentials to cause them to lift off the ring plane [1, 24]. Possible charging mechanisms considered were meteoric impacts or high energy Saturnian auroral electron beams. The sporadic charging events would charge the boulders in the ring to high negative potentials and smaller dust grains on the surface of the boulders be repelled by electrostatic forces. The spokes are typically up to 10,000 km in length and 2000 km in width. The spoke particles are elevated to about 80 km above the ring.

The realization that dust particle dynamics in planetary magnetospheres were influenced by electromagnetic as well as gravitational forces led to the emergence of the field of gravitoelectrodynamics [1,25].

B. Dust streams from Jupiter

In February 1992 the European Space Agency’s spacecraft *Ulysses* flew by the planet Jupiter, at a distance of approximately 5.4 AU from the Sun. This spacecraft was equipped with an instrument capable of detecting dust particles and measuring their masses and impact speeds. Within 1 AU from Jupiter, the detector recorded bursts of dust particles (< 1 μm) in collimated, periodic streams coming directly from Jupiter [26]. Imagine for a moment the impact of this discovery – particles were being *ejected* from the most massive planet in the solar system. This led immediately to two questions: (i) what is the source of these particles, and (ii) what physical mechanism allows these particles to overcome the enormous gravitational pull of Jupiter and be ejected?

The origin of the Jovian dust streams became clear when the NASA spacecraft *Galileo* first approached Jupiter in 1995. The minute dust particles appear to be pumped into the Jovian magnetosphere by active volcanoes on the moon Io. The dust particles acquire an electric charge when they are exposed to the Jovian magnetospheric plasma as well as solar UV radiation. Mihály Horányi of the University of Colorado at Boulder performed a detailed modeling of the dynamics of these particles which include both gravitational and electromagnetic forces as well as a self consistent determination of the dust charge [27]. He found that the grains become positively charged, gain energy from the corotational electric field of Jupiter, and acquire velocities allowing them to escape Jupiter's gravity.

This example was chosen to further illustrate that the dynamics of small dust particles in any solar plasma environment will be strongly affected by electromagnetic and gravitational forces in addition to plasma drag forces and radiation pressure. As Horányi points out, these particles behave as tiny probes of the plasma environment as well as the electromagnetic and gravitational fields of the regions in which they are born and traverse [27]. The charge on a particle is continually changing in response to changes in the plasma environment. In situ measurements of the mass and velocity of these particles can provide otherwise unobtainable information that can be used to verify models of the plasma and planetary environments.

C. Noctilucent clouds and Polar Mesospheric Summer Echoes (PMSE)

Noctilucent clouds (NLCs) are an unusual atmospheric phenomenon that occurs in the high latitude (50°-60°) region of the earth's summer mesosphere. The mesosphere is the region of the earth's atmosphere extending in attitude from 50 to 85 km. The summer mesosphere is the coldest part of the atmosphere, where temperatures drop to *minus* 140°C. NLCs are glowing, silvery clouds that form at an altitude of about 80 km when water vapor condenses into ice particles. These clouds are too thin to be seen in daylight but glow at night just after sunset or just before sunrise when the Sun's rays hit them from below the horizon while the lower atmosphere is still in darkness. Observations of NLCs have been associated with an influx of particulate matter into the atmosphere, and their first reported observations in 1885 were connected to the eruption of Krakatoa. Over the past 40 years NLCs have been getting brighter, increasing in frequency and spreading to latitudes as low as 40°. There has been speculation that the increased occurrence of NLCs might be related to human activity such as pollution from burning of fossil fuels, methane emissions from livestock or even exhaust from the space shuttle about 97% of which is water vapor which ultimately finds its way up to the artic regions.

The location of NLCs coincides with the D region of the lower ionosphere where the plasma density is in the range of $10^3 – 10^4$ cm^{-3}. This means that the ice particles are charged and there is evidence from rocket measurements that the electron density in that region is considerably lower than the positive ion density due to the attachment of electrons on the ice particles, a phenomenon that ionospheric scientists call electron bite-out. NLCs are associated with another unusual phenomenon – polar mesospheric summer echoes or PMSEs first observed by Ecklund and Balsley in 1979 [28]. Ecklund and Balsley observed the backscatter (echoes) of VHF radars from a 50 MHz large dipole antenna array located in Poker Flat, Alaska. These radars are sensitive to 3 m mesospheric structures which produce nonthermal scattering. The mesospheric echoes showed a pronounced seasonal variation in height. During the summer months the echoes showed an unexpected strong peak at about 85 km, whereas in nonsummer months the PMSEs are less intense and occur at lower altitudes of around 55 to 80 km. Fig. 5 is a plot of the seasonal variation of the average height of PMSEs overlaid with the number of displays of NLCs, showing clearly the correspondence between these phenomena.

This correspondence between NLCs and PMSEs means that PMSEs, which can easily be detected from ground radars, are a sensitive indicator of the presence of water vapor in the atmosphere. To the extent that the increase in NLC displays may be connected to anthropogenic activity, the PMSEs can be used as an atmospheric monitoring device. There is also plans to launch a satellite in late 2006 - AIM (Aeronomy of Ice in the Mesosphere) to study polar mesospheric clouds and to reveal if they are possibly caused by global warming, as some scientists suspect.

From the dusty plasma physics point of view, PMSEs and NLCs are an intriguing example of the effects of charging of particles, in this case ice, in a plasma. Although there is no consensus on the mechanism for producing PMSEs, the current thinking is that the enhanced radar backscatter is caused by some irregularity structure in the electron density profile such as steep density gradients. Rocket measurements seem to indicate that the ice particles are

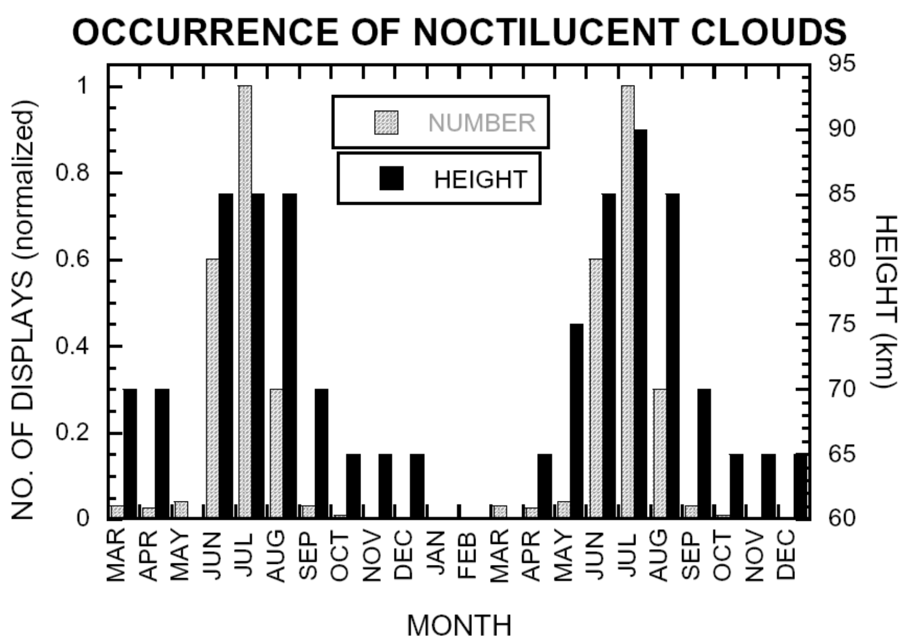

Figure 5. Average height of occurrence of mesospheric echoes and number of displays of noctilucent clouds (normalized) over a two year period.

charged positively [29], even during the night hours when the photoelectric emission of electrons from the ice is not operable. It seems that electrons are attached to very heavy negative ions in this region of the mesosphere, and the charging is dominated by light positive ions. A recent laboratory experiment exploring the dust charging in the presence of heavy negative ions and light positive ions has provided evidence to support this hypothesis [30].

D. Snowy plasmas

One needs not travel to altitudes of 53 miles to find charged ice crystals, they can even be found in the form of charged snow at a mere 10 cm above the ground. Scientists at Montana State University in Bozeman and the U.S. Forest Service in Laramie, Wyoming have measured the charge-to mass ratio of individual blowing snow particles [31]. Charge-to mass ratios as large as -200 μC/kg (negative particles) and +72 μC/kg (positive particles) were determined by measuring the deflection of charged snow as it passed through a region of applied electric field. By comparison, an average size ice crystal of 200 μm diameter immersed in a 1 eV plasma would have a (q/m) ~ -8 μC/kg. The snow gets charged by a process that is generally not important in plasmas but is a common charging mechanism that we are all well aware of – friction (triboelectric charging). Anyone who has suffered an electric shock when touching a door knob after walking across a carpet in the winter has experienced triboelectric charging.

One of the processes by which wind transports particles is saltation – the particles hop along the surface rebounding to heights of about 10 cm of the surface. As a result of the interaction of the bouncing particles with those on the surface both particle can be charged. The bouncing particles are usually negatively charged while the surface particles are positively charged. Of course some of the surface particles may also become airborne so that the blowing particles can be both positive and negative. As a result of this process an electric field develops above the snow surface which can reach values on the order of several kV/m at heights of 10 cm. The blowing particles are thus subject to electrostatic forces as well as gravity and wind drag, and the effects of *charged* snow must also be included in modeling its transport and accumulation. The presence of blowing snow of opposite charge sign also affects how snow builds up on surfaces. The importance of electrostatic forces on charged dust has been considered as a potentially important process in the development of cornices on the edges of mountain slopes which could lead to avalanches.

4. Dusty plasmas in industry

Plasma-based materials processing technologies are widely used in the manufacture of very large scale integrated circuits (VLSI) [9]. Typically, chemically reactive plasmas are applied to sputter, etch or otherwise modify the surface properties of silicon. Surface features 0.2 μm wide and 4 μm deep (trenches) can be etched in silicon films by these processes, and no other commercial technologies exist which can accomplish this. The presence of dust is of critical concern to the microelectronic industry since particle contamination of semiconductor materials was estimated to account for more than 50% of device failures. Dust contamination reduces the yield and performance characteristics of fabricated devices. Simply put, the dust particles fall into the surface features of semiconductors either interfering with the etching process, preventing the adhesion of thin films or contaminating the final product. As the microelectronics industry moved to smaller and smaller structures, the presence of even the smallest dust particles became an urgent issue. The bottom line is that dust contamination adversely affects the ‘bottom line’.

A. Dust contamination in plasma processing devices (dust is a bad thing!)

So where does the dust come from? Initially it was assumed that the semiconductor surfaces were contaminated during handling of the wafers. To alleviate this problem, all fabrication steps were done in clean rooms where particulate levels were carefully monitored. Yet even with the best state-of-the-art clean rooms, semiconductor wafers showed evidence of contamination. It turned out that the surfaces were being contaminated by dust particles actually generated within the processing plasmas. Ironically, this realization was a boom for dusty plasma research, as scientists and engineers scrambled to understand the formation, charging and transport of dust in plasmas and to investigate how the problem might be eliminated, or at least how to minimize its effects.

In order to get a better grasp of the situation it is necessary understand some of the details of how the plasma processing devices work. (These devices are referred to in the industry as ‘reactors’ or ‘tools’ in the sense that the plasma is used to sculpt silicon in the same way that an artist uses a hammer and chisel to sculpt stone.) A typical plasma processing reactor is shown schematically in Fig. 6. This is an rf diode consisting of two parallel circular electrodes, 10-15 cm in diameter and separated by several centimeters. The plasma is produced by applying rf power (0.01 – 1 kW) at a frequency of 13.56 MHz to the diode. (This is the frequency allotted to the industry, and researchers, by the international communication authorities, in the U.S. the FCC.) The feed gas is a combination of a buffer gas, such as argon and up to 10% of a reactive gas such as silane filling the vacuum vessel to a total pressure in the range of 100-500 mTorr. Another gas combination used is

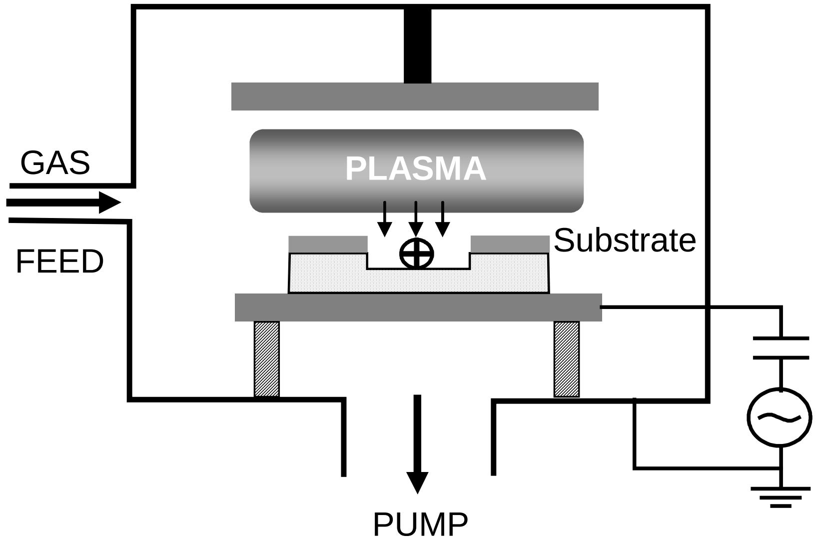

Figure 6. Typical rf plasma diode device used for processing silicon wafers. The feed gas is ionized by applying 13.56 MHz power to the circular, parallel plate electrodes.

O_2/CF_4. This device essentially produces a glow discharge plasma maintained by electron impact ionization of the gas atoms. Usually the upper electrode is grounded and the lower electrode is powered. Since the positive ions cannot respond to the rapidly oscillating rf fields, a negative sheath is developed at the lower electrode.

The substrate which is to be modified is placed on the lower electrode. Etching occurs when the positive ions, accelerated in the sheath potential, bombard the substrate. The process is carried out in a series of steps. The patterns of conductors on the circuit boards and the transistors on microchips are "printed" by first coating the substrate with a material called a photoresist. A photoresist is a polymer coating that is chemically designed to change its properties when exposed to light. The photoresist coating (about 1 μm thick) is selectively radiated (with UV usually) through a stencil or mask allowing the light to fall only on selected areas. The light causes a chemical change in the coating and the irradiated area can then be washed away to expose the underlying substrate. The exposed substrate can then be subjected to the plasma process that etches the trenches. The 'resist' property of the photoresist refers to the fact that it *resists* etching, thus protecting the portions of the substrate where no etching is desired. In the final step the remaining photoresist is removed by applying an appropriate reagent.

The plasma process often involves the use of reactive gases such as silane (SiH_4), methane (CH_4), or dichlorodifluoromethane (CCl_2F_2). As pointed out in Section 2 D, complex plasma-enhanced chemical reactions can take place within these discharges that result in the formation and growth of dust particles. One of the first observations of the presence of dust particles in an rf silane discharge was made by a group in the Chemistry Department at Northwestern University in 1984 [32]. Their discharge was operated with a mixture of argon and 9% silane at a pressure of 0.3 Torr at 5 W of rf power. Light scattering from a pulsed laser at 500 nm revealed sharp spatial peaks of scattered light near electrodes. The location of the scattering peaks correlated well with the plasma sheath edge, where negatively charged particles could be electrostatically trapped. In a similar experiment also using an Ar/SiH_4 gas mixture, Boufendi and Bouchoule at the University of Orleans in France measured the growth of silicon nanocrystals using a combination of transmission electron microscopy (TEM) and laser light scattering. Their results (shown in Figure 2 of this article) showed the formation of particle aggregates with diameters exceeding 50 nm by coagulation. The precursors of these particles are hydrogenated silicon negative ions which are the nucleation centers for the formation of nanocrystallite particles (2 nm) [17].

Perhaps the most spectacular example of trapped dust particles in an rf processing plasma was provided by Gary Selwyn and his colleagues at the IBM Thomas J. Watson Research Center in Yorktown Heights, NY [33]. The IBM experiments were carried out in a commercial rf reactor with a pure argon feed gas and with Si wafers placed on a planar carbon electrode. A video camera was used to image scattered light from particles illuminated with a horizontal sheet of argon laser light that was rastered parallel to the lower electrode by a scanning mirror. This technique allowed a plane of particles to be illuminated and by varying the height of the rastered beam above the rf electrode, a mapping of the spatial distribution of particles could be obtained. A photograph of the scattered laser light is shown in Figure 7. Densely packed particles are seen in continuous rings around the edges of the Si wafers. In addition, a ‘dome’ of particles was over each Si wafer. The particles were trapped in the sheath at the plasma/electrode boundary in electrostatic structures which conform to the topography of the electrode. The wafers were removed from the reactor and an analysis of the particles which had fallen onto the wafers showed a composition of 43% Si, 53% C and 2% N and 2% O. This composition analysis confirmed the suspicion that the particles were formed out of the sputtering products of the wafer and electrode materials. These observations left no doubt that the source of the contamination problem in semiconductor manufacturing was the tool itself.

As a result of these numerous in-depth studies that identified the source of dust contamination, the plasma processing community in the late 1980’s paused to develop research strategies aimed at understanding the basic physics of dusty plasmas. Theoretical, computational and experimental work was directed at the problems of dust formation and growth, charging and transport. Ironically, these technologically driven studies which had as their goal the

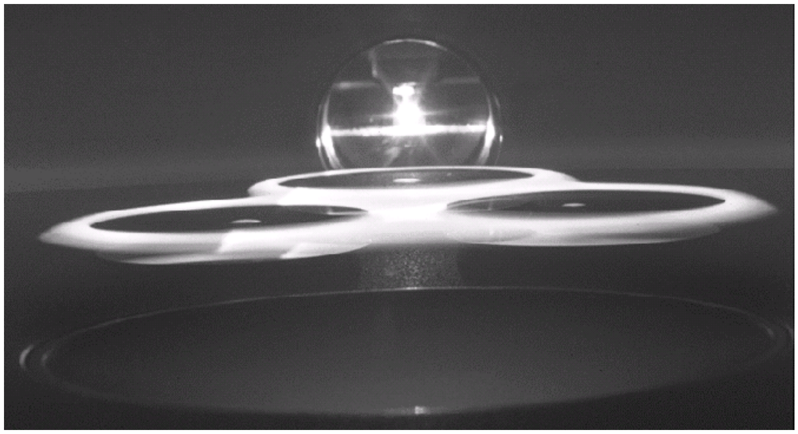

Figure 7. Photograph of rings of dust particles encircling silicon wafers in a plasma processing device. The particles are generated in the plasma. (adapted from [33]).

'elimination' of dust, were going on at about the same time that basic plasma and space physicists, energized in large part by the need to understand the curious spokes in Saturn's B ring, were attempting to devise methods of getting dust into plasmas in order to study its effects. After an initial period of working independently, attending different meetings and publishing their results in different journals, these seemingly disparate groups realized that they tackling the same basic problems and began fruitful communications and interactions. Progress toward understanding the processes of dust formation and growth in the technical area may also help shed light on similar processes in astrophysical environments.

At the present time the dust contamination problem in processing systems is well-controlled. So-called 'clean operation rules' for plasma tools have been developed. These rules are based on the understanding that the negatively charged dust particles would be trapped in potential wells corresponding to local maxima of the time-averaged plasma potential. Some of the dust amelioration strategies that have been developed include:

1. designing tools that prevent the formation of electrostatic traps but rather direct particles toward pumping lines, using for example grooved electrodes,
2. prevent particles from being directed toward the wafer surface when the discharge is terminated,
3. reducing the particle trap efficiency by careful programming the decrease in power before stopping the process,
4. using plasma-induced electrostatic forces to release particles from surfaces,
5. tailoring the gas flow in the reactor to drag the particles into the pumping line.

B. Applications of dusty plasmas (dust is a good thing!)

It didn't take long to realize that the ability to grow dust in a plasma might have useful technological consequences. Dust is no longer considered as an unwanted pollutant, and all of the efforts associated with understanding and reducing its negative impact could be directed in exciting new developments in material science. If we step back for a moment and consider the landscape we see that fine dust particles produced in plasma-chemical systems can have very interesting and useful properties since it is possible to control both their size and composition. Plasmas can not only be used to grow 'designer' particles but can also be used to modify the properties of existing materials that are introduced into the processing plasmas. One of the main advantages of the use of low pressure plasmas is that size of grown particles can be controlled and the very nature of the processes leads to the formation of relatively monodisperse (very narrow size distribution) particles. The nanoparticles grown in plasma discharges are seen as the building blocks of nanotechnology.

A few examples of the applications of dusty plasmas which have already been realized or envisioned are [5, 34]:

1. Nanocrystalline silicon particles grown in silane plasmas, incorporated into the intrinsic layer of amorphous hydrogenated silicon particles (a-Si:H), have been shown to increase both the lifetime and efficiency of silicon solar cells [35]
2. Thin film coating applied in PECVD (plasma enhanced chemical vapor deposition) systems have been applied to materials to improve surface properties. Thin films of TiN in an amorphous Si_3N_4 matrix prepared by PECVD have extremely high hardness and elastic modulus – so-called 'superhard' materials [36].
3. Carbon-based nanostructures grown in hydrocarbon plasmas (methane or acetylene) or fluorocarbons are used to produce amorphous thin carbon films. This can lead to materials having extraordinary properties such as high hardness, chemical inertness, and wear resistance.
4. The production of wear resistant, self-lubricating coatings is currently being investigated. Small lubricating MoS_2 (molybdenum disulfide) particles can be included in a titanium hydride matrix and applied as a coating [37] Over the lifetime of the material as it wears the MoS_2 particles are released and provide a lubricating layer on the material.
5. Nanocrystalline diamond films are routinely fabricated in Ar/CH_4 plasmas [38]. Diamond films have exceptional properties such as high hardness, chemical inertness, and extreme smoothness (low coefficient of friction) have been applied to cutting tools to improve their performance. The high smoothness properties and chemical resistance has also made diamond films attractive as a coating for

optical components. Diamond coatings are also incredibly resistant to erosion due to ion bombardment. Erosion rates 10 times less than molybdenum has been reported. Diamond coatings are being investigated for application in ion thrusters which are being studied as advanced propulsion systems.

6. Diamond whiskers (150 nm in diameter and 200 nm in height) fabricated by etching in rf plasmas have been shown to enhance electron field emission. The reactive ion etching (RIE) process are used to very effectively sharpen the mirco-tips of diamond [39].

These examples were chosen to illustrate the widespread use of dusty plasmas in practical applications. This is a fascinating and exploding field that is truly interdisciplinary in that it combines the expertise of chemists, physicists and engineers, and encompasses worldwide research efforts.

5. Dedicated dusty plasma experiments

In the preceding sections, examples were given of dusty plasmas in which either the dust occurred as a natural part of the environment (planetary rings) or formed out of the constituents of the plasma (rf reactors). In this section we describe dedicated dusty plasma experiments in which dust particles are intentionally introduced into the plasma by various means in order to perform basic experiments. The types of particles that have been used is quite varied ranging from simple powders such as kaolin (used to make pottery) or aluminum oxide (Al_2O_3) to monodisperse spherical glass (SiO_2) or plastic (melamine formaldehyde) particles. The inexpensive powders tend to have large distributions of sizes and are anything but spherical (usually plate-like with irregular boundaries). The monodisperse spherical particles are quite attractive for basic experiments since charging theories tend to assume spherical particles of a given radius, these are however quite expensive. For example, one can purchase 1 gram of melamine formaldehyde spheres of 4.86 $\pm$ 0.07 μm diameter for about $300. Particles can either be of conducting or dielectric materials. Large particles (tens of microns) of graphite, copper or gold are readily available. It is even possible to obtain so-called simulated moon dust, dust which has properties similar to that found in the lunar regolith. Glass micro-balloons – perfect hollow glass spheres are also available, and these have the advantage of being large but not as heavy as solid particles, having an average mass density of about 0.4 g/cm^{-3}. Although these generally come in large batches of various diameters, it is relatively easy to sieve the particles to obtain more well-defined and narrow size distributions.

We will describe some of the experimental devices that have been introduced to study dusty plasmas. Some of the most widely studied dusty plasma issues will also be discussed including dust charging experiments, waves in dusty plasmas, the observation of Coulomb crystals in strongly coupled dusty plasmas, and dusty plasma experiments that have been carried out in the microgravity environment of the International Space Station (ISS). We conclude with a brief description of the potential effects of dust particles found in fusion plasmas.

A. Dusty plasma devices

Except for experiments on the ISS, the dusty plasmas in the lab using micron sized particles will be subject to the dominant force of gravity. The particles will simply fall through the plasma unless some other force (electrostatic, for example) is provided to levitate and confine them. However for many experiments this is not a problem because the typical residence time of a particle in the plasma (a few tenths of a second) is generally very long compared to the time for the particle to become charged, especially for large particles. Thus it is possible to perform interesting experiments by simply sprinkling dust grains into a plasma, in much the same way as one sprinkles salt from a salt shaker.

A typical 'salt shaker' dusty plasma device is shown in Figure 8. The plasma source is a basic hot filament multidipole plasma operating in a vacuum tank of roughly 1 m^3. The chamber is filled with a gas such as argon at a pressure in the range of 10^{-5} – 10^{-3} Torr. Thermionic electrons from a hot tungsten filament are accelerated by a negative discharge voltage, $V_D \approx 40$ - 80 V, and ionize the background neutral gas atoms. The walls of the device are lined with small permanent magnets (multidipoles) to reflect the ionizing primary electrons, increasing their lifetime and thereby greatly enhancing the ionization efficiency. At a discharge current of 1 A and argon pressure of 0.5 mTorr, roughly 0.2% of the neutrals will be ionized. The electron temperature (which is a primary factor in determining the dust charge) is typically in the range of 2 - 5 eV, whereas the ions are generally not much above the temperature of the neutral gas atoms, 0.025 eV.

The salt-shaker or dust dropper is a small (1-2 cm) metal cylinder loaded with dust particles and fitted on the bottom with a fine mesh which only allows particles of a maximum size through. If one wishes to drop just a few particles at a time, the mesh can be replaced with a foil with a pinhole. To disperse the dust, the rod on which the dropper is mounted is struck (either with some handy tool or in more sophisticated versions using an ultrasonic vibrator [40]) allowing the dust to rain down into the plasma. The dust grains can be imaged using a CCD camera and VHS recorder by illuminating them with a laser. A sheet of laser light can be produced using a cylindrical lens. If desired the negatively charged dust can be levitated on a plate below the dropper by applying a sufficiently negative voltage to the plate. The electric field present at the sheath of the plate points downward, producing an upward electrostatic

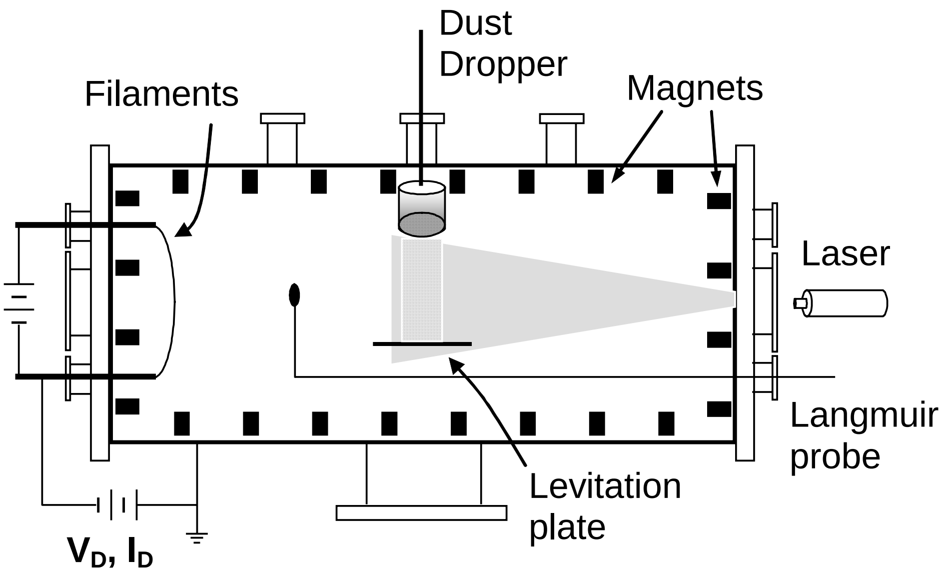

Figure 8. Schematic diagram of a multidipole plasma device and 'salt'shaker' dust dispersal system.

force on a negative particle balancing its weight, mg. This type of device, or similar versions, has been used to measure the charge on individual dust grains [41], to study the effect of dust on plasma waves [40, 42], and to measure the neutral drag forces and ion drag forces on dust particles [43].

A variation of the salt shaker concept was used in conjunction with a Q machine [44] device to produce an extended, steady state, magnetized dusty plasma column [45]. Such a device having a relatively large, extended region of dusty plasma is required to perform investigations of waves in dusty plasmas. A schematic of the dusty plasma device (DPD) is shown in Figure 9.

The DPD utilizes, as the basic plasma source, a Q machine in which a potassium plasma column ~ 5 cm in diameter and ~ 1 m in length is produced by surface ionization of potassium atoms on a tantalum plate heated by electron bombardment to a temperature of ~ 2500 K. The surface is hot enough to emit copious amounts of thermionic electrons, which together with the K^+ ions, form the basic constituents of the plasma. The plasma is confined radially by a uniform longitudinal magnetic field of ~ 0.3-0.5 T. The plasma is relatively cold with ion and electron temperatures $T_i = T_e \approx 0.2$ eV, and plasma densities in the range of $10^8 - 10^{10}$ cm^{-3}. The plasma column is surrounded over the middle $1/3^{rd}$ of its length by a cylinder coaxial with the plasma. The inner surface of this cylinder is lined with aluminum wool which is held in place by a course wire mesh. Dust powder can be loaded into the aluminum wool. The cylinder can be rotated around its own axis, by an external motor and drive assembly up to about 180 rpm. As the cylinder rotates, dust is carried

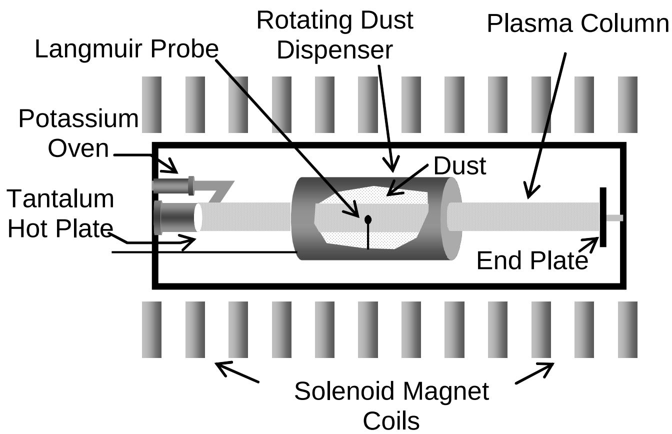

Figure 9. Schematic diagram of a magnetized dusty plasma device, showing the Q machine plasma column, surrounded over a portion of its length by a rotating dust dispenser.

up above the plasma column and allowed to fall through it. The fallen dust is then continuously recycled. Several hundred grams of dust is initially loaded into the cylinder and allows operation over a period of a few days before it must be refilled.

It is important to realize that this device produces magnetized electrons and ions which charges the dust, but the magnetic field is not of sufficient strength to magnetize the dust. This device has been useful in studying the effects of charged dust on various plasma wave modes such as the ion acoustic mode, the electrostatic ion cyclotron mode and instabilities driven by parallel velocity shear. The presence of charged dust modifies the dispersion properties of plasma waves as well as their excitation conditions as detailed in references [4] and [7].

Dusty plasmas have also been produced using a positive column plasma of the type not unlike J. J. Thompson used in his discovery of the electron. A schematic of this is shown in Figure 10.

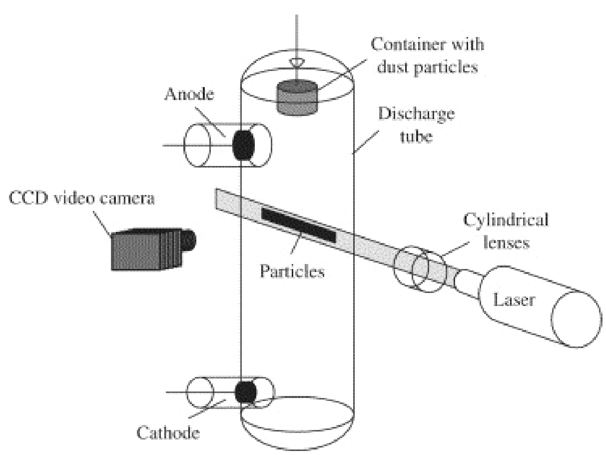

Figure 10. Schematic of a positive column dust plasma device. Reprinted with permission of A. Ivlev [9].

The discharge tube is filled with a noble gas in the range of 0.1- 1 Torr. A glow discharge is formed when a DC potential of ~ 200-300 V is applied between the cathode and anode. A dust dropper located at the top of the tube allows dust to fall through the plasma. The positive column discharge is characterized by regions (striations) of periodic changes in the density and potential along the axis of the discharge tube. When standing strata are formed it is possible to trap dust grains in these regions since they are regions of higher plasma potential. This type of device was used by V. E. Fortov and his colleagues at the High Energy Density Research Center in Moscow to observe ordered structures of micron sized dust particles confined in the striations of neon glow plasmas [46].

A device which also utilizes a plasma having regions of positive plasma potential (a double layer with relatively strong electric field) to trap dust is shown in Figure 11 [47]. The vacuum chamber is filled with nitrogen or argon gas at a pressure of ~ 100 mTorr. A glow discharge is produced by applying + 300 – 400 V to a 3 cm anode disk located on the axis of the chamber. Dust is introduced into the plasma by placing a rectangular metal tray about 3 cm below the anode disk. About 25 g of kaolin powder (aluminum silicate) is spread over the tray. When the discharge is turned on, some of the dust is attracted into the discharge where it is trapped electrostatically. Light scattered from the dust could be easily seen on a video camera. This device has been used to investigate the dispersion properties of dust acoustic waves, Dust acoustic (DA) waves are basically sound waves which propagate through the dust component of a dusty plasma. This is the first example of a "dust" wave and was discovered theoretically by Shukla and first discussed in 1989 at the First Capri Workshop on dusty plasmas with the details published in 1990 by Rao, Shukla and Yu [48].

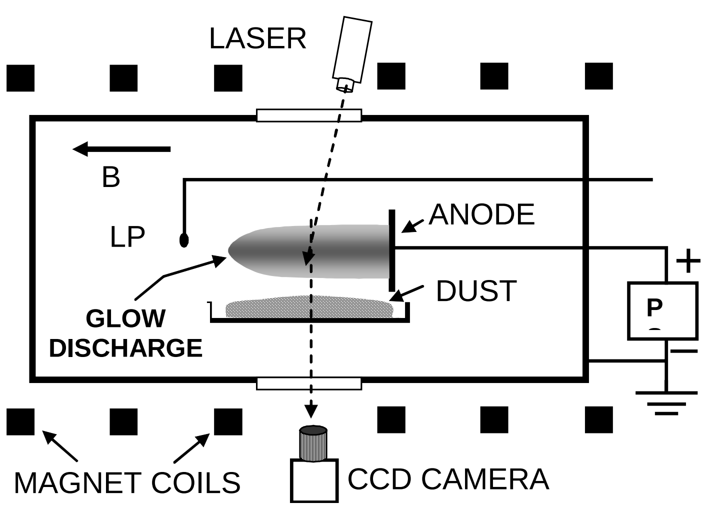

Figure 11. Schematic of a magnetized glow discharge dusty plasma. Dust particles are lifted up into the glow discharge when it is initiated by applying a DC voltage to an anode disk immersed in argon. The dust is confined (levitated) by strong electric fields within the anode glow.

Since the dust is one of the charged fluid components of the plasma, it can support wave modes in the same way that an ordinary plasma supports ion acoustic waves. The DAW is a compressional disturbance which propagates through the dust and directly involves the dynamics of the dust particles. Since the dust particles are relatively massive, it is a very low frequency wave, just a few Hz typically and propagates at a speed of a few cm/s. This wave is spontaneously excited in the plasma due to ions drifting relative to the dust. The wave can be easily observed by imaging the dust particles as shown in Figure 12.

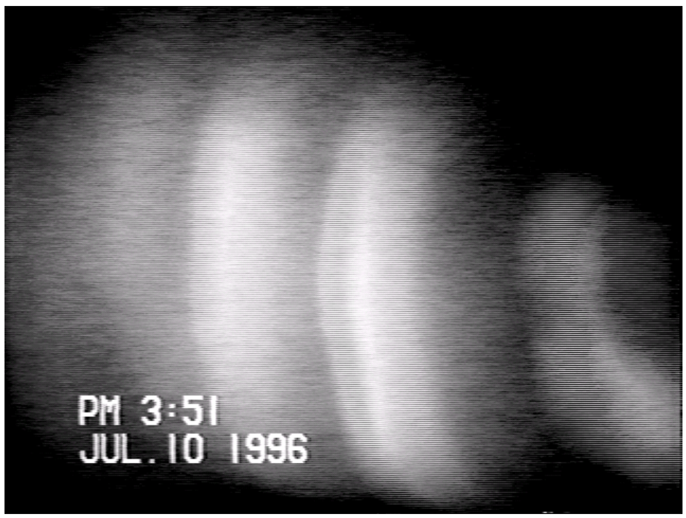

Figure 12. Single frame video image of a dust acoustic wave in a DC glow discharge plasma. (from ref [47])

In this image the anode disk is on the right side and the 30 Hz wave is propagating from right to left at a phase speed of 12 cm/s. The bright vertical bands of light in the image correspond to regions of dust compression. A wavelength of ~ 4-5 mm is inferred by measuring the separation between these wavefronts. The dispersion properties of the DAW depend sensitively on the particle size. Uwe Kortshagen of the University of Minnesota has proposed using the DAW during the dust nucleation phase of the plasma in a PECVD system as a diagnostic for nanometer-sized particles [49].

B. Coulomb crystals

As pointed out in Section 2 C, Ikezi speculated 20 years ago that highly charged dust grains in a plasma might form an ordered structure or Coulomb crystal [15]. This was realized in 1994 when three groups reported observations of two-dimensional Coulomb (also known as dust crystals or plasma crystals) [50]. Serendipitously, the experimental demonstration of Coulomb crystals followed on the accidental discovery of Selwyn [33], that charged dust grains were levitated in the sheath at the lower electrode of an rf diode. In order to study the dust contamination problem in processing devices, a standardized device was developed for generating rf plasmas in various gases at 13.56 MHz. This design for this reference chamber was developed at the 1988 Gaseous Electronics Conference and is known as the GEC Cell [51]. The basic configuration for this device is shown in Fig. 6. This design or slight variations were adopted by numerous groups around the world and was instrumental in the discovery of Coulomb crystals. With this device, Coulomb crystals can easily be formed and their properties measured using laser light scattering techniques.

A typical setup used to produce Coulomb crystals is shown in Figure 13. Monodisperse dust particles are sprinkled into the rf diode using a retractable dust dropper. The particles are levitated in the sheath above the lower electrode. Horizontal confinement of the negatively charged dust particles is provided by a radial electric that is naturally present in the device and which can be enhanced by placing a copper ring (few mm height) above the lower electrode. The particles are illuminated using a fan shaped sheet of laser light which is scattered into the field of view of a CCD camera which images the particle array through a hole in the upper grounded electrode.

An image of a typical dust crystal is shown in Figure 14. The dust particles are arranged in a single horizontal layer with a hexagonal crystal structure. Dust crystal formation requires highly charged particles (Q/e ~ 10,000), which are cooled to room temperature by interaction with the neutral gas. The Coulomb coupling parameter (Eq. 16) for these crystals is usually ~1000 or higher. Recently, fully three dimensional “Coulomb balls” have also been observed [52].

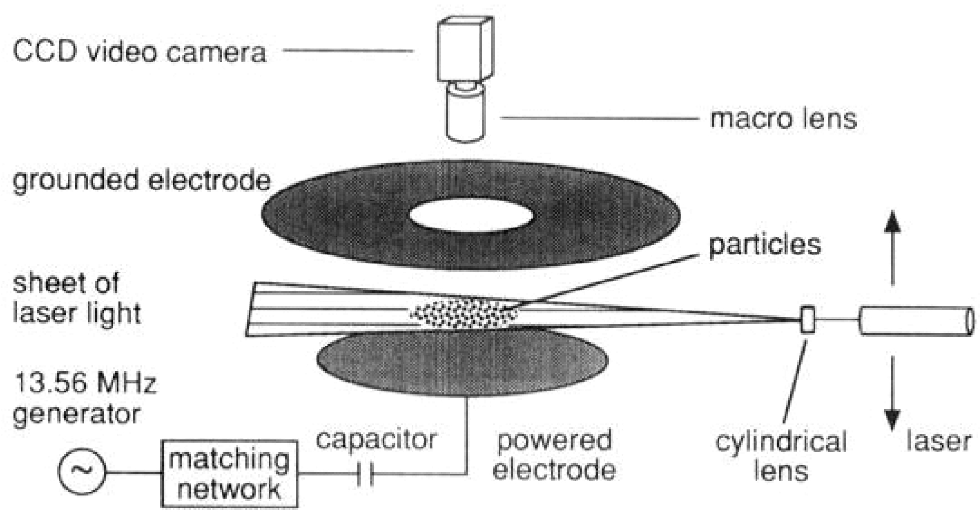

Figure 13. Schematic diagram of the apparatus used to produce Coulomb crystals.

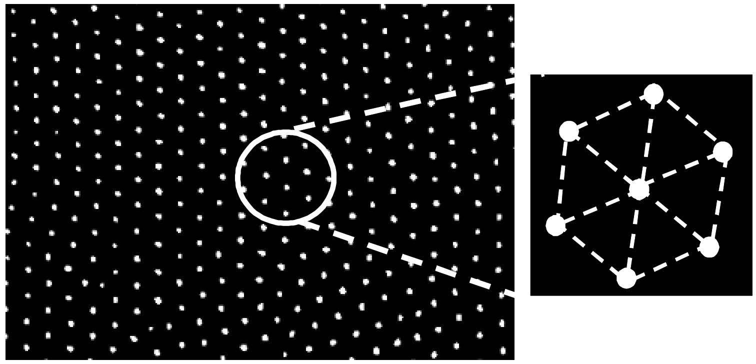

Figure 14. Two-dimensional Coulomb crystal with hexagonal structure.

The discovery of Coulomb crystals, which have been referred to new states of matter, has opened up entirely new areas of investigation. Unlike colloidal systems, the dust structures form on rapid timescales and are easily imaged. Laser diagnostic techniques allow researchers to follow the full dynamics of these systems at the kinetic level. The ability to follow the positions and velocities of all particles in the system is unprecedented and provides a view that is generally not possible in many-particle systems. Researchers have been able to probe the solid-liquid phase boundary in these systems by studying the conditions that lead to more disordered states or melting [53].

So far, there have been very few suggestions of how or where dust crystals might be applicable outside the laboratory. Recently, however an exciting technical application was analyzed by Marlene Rosenberg, Dan Sheehan and Padma Shulka [54]. They considered the potential use of dust crystals as *tunable* filters for electromagnetic radiation at terahertz (THz) frequencies. The idea is to use the dust crystal as a Bragg diffraction grating. The Bragg condition related the wavelength of the electromagnetic radiation, λ to the distance, d between planes in the crystalline array: $\lambda = 2d \sin\theta$. For example, for a wave at 3 THz, λ = 100 μm, and with $\theta = \pi/2$, the Bragg condition requires a d = 50 μm. Lattice spacings on this order is typical for a dust crystal. Furthermore, the spacing of the lattice planes d is a function of plasma and dust parameters, so that the dust crystal filter is tunable.

C. Dusty experiments onboard the International Space Station (ISS)

The fact that the Coulomb crystals produced in the laboratory are comprised of at most a few layers and are planar is a consequence of gravity. The downward pull of gravity on the particles is only arrested a few millimeters above the lower electrode where the downward electric field in the sheath is strong enough to levitate them. Gravity effectively squeezes the particles into compressed pancake-like structures. In an attempt to isolate the real interactions between the particles and other plasma effects, dusty plasma experiments in the microgravity environment provided first on the Russian MIR station and now on the International Space Station (ISS) were undertaken. These experiments were conceived and carried out as part of a joint effort by the Max Planck Institute for Extraterrestrial Physics (MPE) and the Russian Academy of Sciences. Details of these ambitious experimental campaigns can be found in two papers published in the New Journal of Physics [55].

One of the primary motivations for microgravity experiments was the realization that with the elimination of the largest force on the particles (gravity), the effects of smaller forces, such as the particle-particle interaction and ion-dust interaction (ion drag) could be investigated. Furthermore, the expectation was that in microgravity the dust structures would no longer be squashed down into 'dust crepes'. The basic experimental setup used was the rf diode built into a package of instruments and diagnostics called he PKE-Nefedov (Plasma Kristal Experiments). The experiments were very successful in producing fully three–dimensional dust structures in this relatively stress–free environment, as shown in Figure 15.

The microparticles were identified in a single video frame and then followed in time to reveal their dynamical behavior. Several interesting features can be identified in this image: (i) a microparticle–free void in the center with a sharp boundary to the dusty plasma, (ii) stable and regular crystalline structures along the vertical central axis, and (iii) vertical motions along the horizontal axis and corners. Several coexisting crystal structures were observed in the microgravity environment – fcc (face–centered cubic), bcc (body–centered cubic) and hcp (hexagonal close–packed). This was the first time that the theoretically predicted bcc phase was observed.

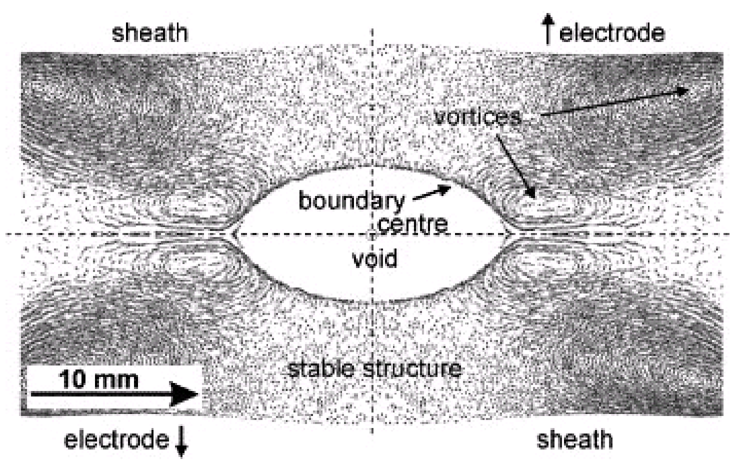

Figure 15. Typical image of a dust cloud obtained in the PKK-Nefedov experiment onboard the ISS. The cloud is composed of 6.4μm particles and completely fills the cylindrical volume between the upper and lower electrodes. The image shows a vertical slice of the particle cloud which is illuminated by a vertical sheet of laser light [9].

The dust−free region, or *void* in the center of the dust cloud was an unexpected and somewhat ironic result. It results from the fact that in the absence of gravity, the ion drag force becomes one of the dominant forces on dust particles. The plasma potential in these discharges has a maximum in the center, thus there is an outward pointing electric field which causes the positive ions to have a net outward flow. As the ions move outward they 'drag' the dust particles with them, forming a dust−free void in the center. The void boundary occurs where the electric and ion drag forces are balanced. Void formation can be circumvented by operating at low plasma densities, where the ion drag force (proportional to n_i) is smaller [56].

D. Dust in fusion devices

We conclude this section on dusty plasmas in the laboratory with a brief account of the realization and consequences of dust in fusion devices. One of the early voices in pointing out this new challenge to nuclear fusion research was Jörg Winter of the Ruhr University in Bochum, Germany [57]. The issues are: (a) what is the source of the dust, and (b) what are its potential affects? The presence of dust in tokamaks is a result of the strong interaction between the material walls and the energetic plasma particles. Dust particles of 10 nm to 100 μm appear to be present in all fusion devices in addition to larger flakes up to millimeters. The particles are composed mainly of materials that directly face the plasma, so called plasma−facing components (PFC) [58]. Average dust mass densities found on surfaces in fusion devices as high as 1000 mg/m^2 have been reported [58]. Mechanisms for dust production in tokamaks that have been identifies include: surface flaking, blistering, arching and erosion of carbon limiters. Plasma−surface interactions in the next major international fusion project, ITER, are expected to be even more intense, resulting in even larger quantities of dust than those found in present devices.

One of the major concerns associated with a large dust inventory is that the dust may retain significant amounts of tritium. The tritium in the dust will not be reprocessed leading to an increase in its inventory over time. The danger is that in an accident, dust would be a carrier for tritium. The presence of hydrogen in the dust in itself poses an explosion hazard. Apart from these important safety concerns, there is the issue of the effect of the dust on the plasma. It is know that the dust does not remain where it was produced but can migrate around during the plasma discharge. Simulations of dust dynamics in fusion devices indicates that dust transport can lead to deep penetration toward the plasma core [58, 59]. Small charged dust particles can be trapped on magnetic field lines of toroidal plasmas, allowing them almost unlimited access to all regions of the plasma. Evaporation of this dust can lead to potentially deleterious impurity problem within the plasma.

The history of fusion research reveals many challenges that needed to be overcome both to our physical understanding of plasma behavior as well as to the practical engineering issues of bringing large, complex devices on line. Apparently, the presence of dust in these devices is providing new challenges that are presently being vigorously addressed by the fusion science community, which is relying on and benefiting from the roughly 20 years experience of the dusty plasma community. As pointed out by Winter, the dust in fusion device problem provides for an interesting connection between low- and high-temperature plasma physics [60].

6. Summary

This Chapter has presented a brief review of dusty plasma research and applications, with examples taken from space, the laboratory and industry. The author hopes to have conveyed the idea that dusty plasmas are rather ubiquitous and probably far less rare than the rather pristine ensemble of electrons and protons. Dust particles seem to find their way into plasmas either as an impurity present in the vacuum system, sputtered off of the walls by energetic particles, or actually created and grown in the plasma by complex plasma-chemical processes. The most important point to realize about dust in plasmas is that it will be electrically charged. Thus the location and distribution of dust particles in a plasma will be determined by the combined effects of gravity, electric and magnetic forces, and the interaction forces with neutral atoms and molecules and plasma ions and electrons, some of which depend on the dust charge. Typically due to the higher thermal speed of the electrons, the microparticles will be negatively charged, but the charging process can be considerably more complicated in plasmas having energetic electrons or ions due to secondary emission. Dust particles bathed in UV radiation (e.g. sunlight) can acquire a positive charge due to the emission of photoelectrons. In the Introductory section of this chapter several examples of dusty plasmas were given (see Table 1). These examples included both naturally occurring dusty plasmas and dusty plasmas that are connected to various man–made activities.

The basic physical principles governing the formation and behavior of dusty plasmas was presented in Section 2 A. The method for calculating the charge on a dust grain under various ambient conditions was discussed. The dust grains are modeled as spherical capacitors of radius a, with the charge given by $Q = C\,\phi_s$, where ϕ_s is the potential of the dust grain relative to the plasma potential, and $C = 4\pi\varepsilon_o a$. ϕ_s is determined from the fact that the dust grains are electrically floating, as expressed in the charging equation (Eq. 1).

The forces on dust grains in a plasma were considered in Section 2 B. The main forces acting on dust are gravity (Eq. 5), the electric force (Eq. 6), neutral drag force (Eq. 7), thermophoretic force (Eq. 8) and the ion drag force (Eqs. 9–15). These forces largely determine how the dust migrates and where it may or may not finally reside in the plasma. One of the most novel aspects of a dusty plasma is that due to the very large charge on the dust, the interaction between nearest neighbor dust grains can be very strong, unlike the relatively weak interactions of electrons and ions in an ordinary plasma. This strongly coupled nature of dusty plasmas is described in Section 2 C, and the Coulomb coupling parameter Γ, which quantifies the strength of the interaction, is defined in Eq. 16. Finally, in Section 2 D the physio–chemical mechanisms through which dust particles can actually be formed and grow to micron sized particles is briefly presented.

The balance of this chapter provided a more in–depth account of dusty plasmas in three different contexts. In Section 3 details of dusty plasmas in the solar system and in the earth's environment were presented. The spectacular discovery of spokes in Saturn's B ring by the Voyager spacecraft was discussed in Section 3 A. The transient nature of these spokes demanded an explanation that took into account electromagnetic effects on charged dust particles. This discovery was one of two watershed events that boosted dusty plasma research in the 1980's. Section 3 B provides an account of the equally astonishing observation of dust streams emanating from Jupiter. This is another prime example of the interplay of gravitational and electromagnetic forces on charged dust in the solar system.

Closer to earth, are the Noctilucent clouds (NLCs) and polar mesospheric summer echoes (PMSEs), described in Section 3 C. These are unusual atmospheric effects connected with charged ice particles in the earth's mesosphere, at about 85 km altitude. The 'echoes' refers to unusually strong radar backscattering which is not completely understood, but are thought to be connected to electron density anomalies associated with the charged ice. Section 3 D described the peculiar example of 'snowy' plasmas, caused by the frictional charging of blowing snow. It is curious to speculate that anyone who has had the misfortune to experience a blizzard has been literally in a dusty plasma.

Dusty plasmas in industry was the subject of Section 4. Here practical issues become paramount depending on whether the dust is considered an unwanted contaminant in the plasma or whether it can be used in novel material science applications. Here again, the science of dusty plasmas was propelled forward by unexpected discoveries that proved to be another watershed event in dusty plasma research. In particular, scientists and engineers discovered, inadvertently, that particles which were contaminating silicon wafers in plasma processing tools were actually produced within the plasma. Details of these findings and the successful efforts to overcome this problem were summarized in Section 4 B. The realization of the potential uses of custom manufactured dust in plasmas, and some of the technical applications that are being explored were discussed in Section 4 B.

One should not loose sight of the fact that although the elimination of dust in plasmas was a primary concern in the semiconductor processing industry, the efforts to understand dusty plasmas and the development of tools to study them greatly advanced dusty plasma science leading to further scientific discoveries, some of which were discussed in Section 5. Section 5 A was an introduction to some of the basic laboratory devices that were developed in the early 1990's to perform dedicated experiments. In these devices, dust was intentionally introduced in order to study the charging mechanisms, the forces on dust grains, dusty plasma waves and instabilities, and strongly coupled systems or dust crystals. These devices incorporated existing plasma sources such as hot filament discharges, DC and rf glow discharges, and Q machines. It turned out that getting dust into a plasma was not all that difficult. It could simply be dispersed using simple salt shaker-type gadgets. Since theoretical work on dusty plasmas had a good head start, the introduction of these experiments was essential in order to provide benchmarks for the theories. The formation of ordered structures of dust particles or dust crystals in strongly coupled dusty plasmas was one of the most exciting developments in dusty plasma research and these findings were described in Section 5 B.

Recognizing the desirability of eliminating the force of gravity on dust particles, which is often dominant, researchers took advantage of the possibility of performing experiments onboard both the Russian MIR space station and now the International Space Station (ISS). The hope was that with the removal of the stresses imposed by gravity, it might be possible to achieve fully three dimensional strongly coupled dusty plasmas, and observe the effects of dust-plasma interactions that were otherwise masked in earth-based devices. The results, which were summarized in Section 5 C, again showed certain surprises (e.g., dust-free voids and vortices), but confirmed the prediction that relatively large, stable 3D dust structures could be produced in the microgravity environment. Even as this chapter was being written, the NASA space shuttle Discovery, as part of mission STS-121, was transporting German born European Space Agency (ESA) astronaut Thomas Reiter to the ISS, where he will carry out new dusty plasma experiments on the PK-4 device, a combined DC/rf discharge.

Finally Section 5 D provided a few details of potential problems associated with the presence of dust in fusion devices. This is another example of the undesirable presence of dust produced, in this case, by strong plasma-surface interactions within the vacuum vessel. Attempts to deal with this issue as the ITER project goes forward is providing new challenges to the dusty plasmas community that will undoubtedly advance our understanding of how charged dust particles, subject to both electric *and* magnetic forces, behave in high temperature plasmas.

Acknowledgments

This work was supported by the U. S. Department of Energy under grant No. DE–FG02–04ER54795.

References

1. Goertz, C. K., 1989, Rev. Geophys. 27, 271.
2. Mendis, D. A., 2002, Plasma Sources Sci. Technol. 11, A219.
3. Shukla, P. K., 2001, Phys. Plasmas 8, 1791.
4. Shukla, P. K. and Mamun, A. A., 2002, Introduction to Dusty Plasma Physics, IOP, Bristol.
5. Bouchoule, A., 1999, Dusty Plasmas, Physics, Chemistry and Technological Impacts in Plasma Processing, A. Bouchoule, Ed., John Wiley, Chichester.
6. Piel, A. and Melzer, A., 2002, Plasma Phys. Control. Fusion 44, R1.
7. Verheest, F., 1996, Space Sci. Rev. 77, 267.
8. Fortov, V. E., Ivlev, A. V., Khrapak, S. A., Khrapak, A. G., and Morfill, G. E., 2005, Physics Rep. 421, 1.
9. Lieberman, M. A. and Lichtenberg, A. J., 2005, Principles of Plasma Discharges and Materials Processing, Second Ed., Wiley Interscience, Hoboken, N. J.
10. Merlino, R. L, and Goree, J. A., 2004, Physics Today July 2004, 32.
11. Allen, J. E., 1992, Physica Scripta 45, 497.
12. Barnes, M. S., Keller, J. H., Forster, J. C., O’Neill, J. A., and Coultas, D. K., 1992, Phys. Rev. Lett. 68, 313.
13. Rothermel, H., Hagl, T., Morfill, G.E., Thoma, M.H., and Thomas, H.M., 2002, Phys. Rev. Lett. 89, 175001.
14. Khrapak, S.A., Ivlev, A. V., Zhdanov, S.K., and Morfill, G. E., 2005, Phys. Plasmas 12, 042308.
15. Ikezi, H., 1986, Phys. Fluids 29, 1764.
16. Praburam G., and Goree, J., 1996, IEEE Trans. Plasma Sci. 24, 97.
17. Bouchoule, A. and Boufendi, L., 1993, Plasma Sources Sci. Technol. 2, 204; Boufendi, L. and Bouchoule, A., 1994, Plasma Sources Sci. Technol. 3, 262.
18. De Bleecker, K., 2006, Ph. D. Thesis, University of Antwerp.
19. Spitzer, L., 1978, Physical Processes in the Interstellar Medium, John Wiley, N. Y.
20. Alfvén, H. and Arrhenius, G., 1976, Evolution of the Solar System, NASA publication SP–345, NASA, Washington, D. C.
21. Smith, B. A., et al., 1982, Science 215, 504.
22. McGhee, C. A., French, R. G., Dones, L., Cuzzi, J. N., Salo, H. J., amd Danos, R., 2005, Icarus 173, 508.
23. Mitchell, C. J., Hoŕanyi, M., Havnes, O., and Porco, C. C., 2006, Science 311, 1587.
24. Hill, C. J. and Mendis, D. A., 1980, Moon and Planets 23, 53.
25. Morfill, G. E., and Grün, E., 1979, Planet, Space Sci. 27, 1269; Northrop, T. G., 1992, Physica Scripta 45, 475.
26. Grün, E., et al., 1993, Nature 362, 428; Hoŕanyi, M., 2000, Phys. Plasmas 7, 3847.
27. Hoŕanyi, M., Morfill, G., and Grün, E.,1993, Nature 363, 144.
28. Ecklund, W. L., and Balsley, B. B., 1981, J. Geophys. Res. 86, 7775.

29. Rapp, M., Hedin, J., Strelnikova, I., Friedrich, M. Gumbel, J., and Lübken, F.-J., 2005, Geophys. Res. Lett. 32, L23821.
30. Kim, Su–H. and Merlino, R. L., 2006, Phys. Plasmas 13, 052118.
31. Schmidt, D. S., Dent, J. D., and Schmidt, R. A., 1998, Annals of Glaciology 26, 207.
32. Roth, R. M., Spears, K. G., Stein, G. D., and Wong, G., 1985, Appl. Phys Lett. 46, 253.
33. Selwyn, G. S., Heidenreich, J. E., and Haller, K. L., 1991, J. Vac. Sci. Technol. A 9, 2817.
34. Boufendi L. and Bouchoule, A., 2002, Plasma Sources Sci. Technol. 11, A211.
35. Cabarrocas, P. R., Chaâbane, N., Kharchenko, A. V., and Tchakarov, S., 2004, Plasma Phys. Control. Fusion 46, B235.
36. Vepřek, S. Reiprich, S., and Shizhi, L., 1995, Appl. Phys. Lett. 66, 2640.
37. Stoffels, E., Stoffels, W. W., G., Ceccone, G., Hasnaoui, R., Keune, H., Wahl, G., and Rossi, F., 1999, J. Appl. Phys. 86, 3442.
38. Zhou, D., McCauley, T. G., Qin, L. C., Krauss, A. R., and Gruen, D. M., 1998, J. Appl. Phys. 83, 540.
39. Tyler, T., Zhinov, V. V., Kvit, A. V., Kang, D., and Hren, J. J., 2003, Appl. Phys. Lett. 82, 2904.
40. Nakamura, Y., and Bailung, H., 1999, Rev. Sci. Instrum. 70, 2345.
41. Walch, B., Hoŕanyi, M., and Robertson, S., 1995, Phys. Rev, Lett. 75, 838.
42. D'Angelo, N., 1990, Planet. Space Sci. 38, 1143; Merlino, R. L., Barkan, A., Thompson, C and D'Angelo, N., 1998, Phys. Plasmas 5, 1607.
43. Hirt, M., Block, D. and Piel, A., 2004, Phys. Plasmas 11, 5690.
44. Motley, R. W., 1975, Q Machines, Academic Press, San Diego.
45. Xu, W., Song, B., Merlino, R. L., and D'Angelo, N., 1992, Rev. Sci. Instrum. 63, 5266.
46. Fortov, V. E., Nefedov, A. P., Torchinsky, V. M., Molotkov, V. I., Petrov, O. F., Samarian, A. A., Lipaev, A. M., and Khrapak, A. G., 1997, Phys. Lett. A. 229, 317.
47. Thompson, C., Barkan, A., D'Angelo, N., and Merlino, R. L., 1997, Phys. Plasmas 4, 2331.
48. Rao, N. N., Shukla, P. K., and Yu, M. Y., 1990, Planet. Space. Sci. 38, 543.
49. Kortshagen, U., 1997, Appl. Phys. Lett. 71, 208.
50. Morfill, G, E., and Thomas, H., 1996, J. Vac. Sci. Technol. A 14, 490; Morfill, G. E., Ivlev, A. V., Khrapak, S. A., Klumov, B. A., Rubin–Zuzic, M., Konopka, U., and Thomas, H. M., 2004, Contrib. Plasma Phys. 44, 450.
51. Hargis, P. J., et al., 1994, Rev. Sci. Instrum. 65, 140.
52. Arp, O., Block, D., Piel, A., and Melzer, A., 2004, Phys. Rev, Lett. 93, 165004.
53. Lin, I., Juan, W.-T., Chiang, C.-H., and Chu, J. H., 1996, Science 272, 1626; Thomas, H. M. and Morfill, G. E., 1996, Nature 379, 806; Melzer, A., Homann, A. and Piel, A., 1996, Phys. Rev. E 53, 2757.
54. Rosenberg, M., Sheehan, D. and Shukla, P. K., 2006, IEEE Trans. Plasma Sci. 34, 490.
55. Mikikian, M., Boufendi, L., Bouchoule, A., Thomas, H. M., Morfill, G. E., Nefedov, A. P., Fortov, V. E., and the PKE–Nefedov team, 2003, New J. Phys. 5, 19.1; Nefedov, A. P., et al. 2003, New J. Phys. 5, 33.1.

56. Rothermel, H., Hagl, T., Morfill, G. E., Thoma, M. H., and Thomas, H. M., 2002, Phys. Rev. Lett. 89, 175001.
57. Winter, J., 1998, Plasma Phys. Control. Fusion 40, 1201; 2000, Phys. Plasmas 7, 3862.
58. Pigarov, A. Y., Krasheninnikov, S. I., Soboleva, T. K., and Rognlien, T. D., 2005, Phys. Plasmas 12, 122508.
59. Krasheninnikov, S. I., Tomita, Y., Smirnov, R. D., and Janev, R. K., 2004, Phys. Plasmas 11, 3141.
60. Winter, J., 2004, Plasma Phys. Control. Fusion 46, B 583.